Bioinspiration &
Biomimetics

PAPER • **OPEN ACCESS**

Powering a molecular delivery system by harvesting energy from the leaf motion in wind

To cite this article: Serena Armiento *et al* 2025 *Bioinspir. Biomim.* **20** 016023

IOP Publishing Bioinspir. Biomim. 20 (2025) 016023 https://doi.org/10.1088/1748-3190/ad98d3

Bioinspiration & Biomimetics

OPEN ACCESS

RECEIVED
4 July 2024

REVISED
5 November 2024

ACCEPTED FOR PUBLICATION
29 November 2024

PUBLISHED
19 December 2024

PAPER

Powering a molecular delivery system by harvesting energy from the leaf motion in wind

Serena Armiento[1,4], **Iwona Bernacka-Wojcik**[2,4], **Abdul Manan Dar**[2], **Fabian Meder**[1,3,*], **Eleni Stavrinidou**[2,*] and **Barbara Mazzolai**[1,*]

[1] Bioinspired Soft Robotics (BSR), Istituto Italiano di Tecnologia (IIT), Via Morego 30, 16163 Genova, Italy
[2] Laboratory of Organic Electronics, Department of Science and Technology, Linkoping University, Norrköping 601 74, Sweden
[3] Surface Phenomena and Integrated Systems, The BioRobotics Institute, Scuola Superiore Sant'Anna, Via C. Maffi 27, 56126 Pisa, Italy
[4] These authors contributed equally.
[*] Authors to whom any correspondence should be addressed.

E-mail: fabian.meder@santannapisa.it, eleni.stavrinidou@liu.se and barbara.mazzolai@iit.it

Keywords: OEIP, TENG, biohybrid, energy harvesting

Supplementary material for this article is available online

Abstract

Smart agriculture tools as well as advanced studies on agrochemicals and plant biostimulants aim to improve crop productivity and more efficient use of resources without sacrificing sustainability. Recently, multiple advanced sensors for agricultural applications have been developed, however much less advancement is reported in the field of precise delivery of agriculture chemicals. The organic electronic ion pump (OEIP) enables electrophoretically-controlled delivery of ionic molecules in the plant tissue, however it needs external power-supplies complicating its application in the field. Here, we demonstrate that an OEIP can be powered by wind-driven leaf motion through contact electrification between a natural leaf and an artificial leaf. This plant-hybrid triboelectric nanogenerator (TENG) directly charges the OEIP, enabling proton delivery into a pH indicator solution, which triggers visible color changes as a proof-of-concept. The successful delivery of up to 44 nmol of protons was revealed by pH measurements after 17 h autonomous operation in air flow moving the plant and artificial leaves. Several control tests indicated that the proton delivery was powered uniquely by the charges generated during leaf fluttering. The OEIP-TENG combination opens the potential for targeted and self-powered long-term delivery of relevant chemicals in plants, with the possibility of enhancing growth and resistance to abiotic stressors.

1. Introduction

Precision agriculture holds great potential to feed a growing global population via optimization of resources management. Leveraging advanced sensing technologies and analytics, farmers might be able to get detailed and real-time information on the plant health status, thus leading to increased profitability and more efficient use of resources [1, 2]. Recently, a variety of advanced and low cost sensors for crop health, soil status, and environmental conditions have been developed [3, 4]. The acquired sensor data should be converted into actionable responses to enable fine-tuning of various agricultural operations, such as watering and application of fertilizers or plant biostimulants [5, 6]. However, the field of smart delivery devices for agrochemicals has only started to emerge recently. The most common conventional methods for chemicals delivery, i.e. soil application and foliar spraying, suffer from very low efficiency and can potentially lead to phyto- and environmental toxicity [6–8]. Novel approaches for the delivery of chemicals are evolving. For example, nanoparticle encapsulation aims to release nutrients/pesticides in a slow, controlled manner [7, 9, 10]. The smart nanocarrier systems possess the potential for controlled release of fertilizers and pesticides in response to customized environmental triggers [11, 12]. The organic electronic ion pump (OEIP), on the other hand, enables fine tuning and dynamic control of the

molecule delivery due to its electrophoretic principle [13–20]. The OEIP consists of a delivery channel filled with an ion exchange membrane (i.e. polyelectrolyte of opposite charge to the delivered ions) connected to the source reservoir. Under application of an electric field, ions from the OEIP source reservoir are delivered to target tissues [20, 21]. Ion flux depends on both the concentration gradient and the electric field, as described by the Nernst–Planck equation. In electrophoretic drug delivery, the flux, or number of molecules delivered, is directly related to the current, which is proportional to the applied voltage. As voltage increases, so does the current, driving more charged molecules across the medium per unit of time. Therefore, higher voltages increase the number of molecules that can be delivered in each time period as long as devices are operated below the limiting current range [21, 22]. The delivery of counter-ions is selective as the transport of co-ions from the target is highly reduced due to the high-fixed charge concentration of the polyelectrolyte. As the delivery is electronically controlled, it can be precisely modulated and triggered by sensor inputs. Particularly in plant biology, the OEIP was demonstrated to bioelectronically control plant stress response and plant growth via delivery of phytohormones such as abscisic acid, auxin and cytokinin [18–20, 23]. However, the OEIP requires an external power supply, which is a major issue for its application in agriculture, where low-cost and portable systems are required. Recently, it was demonstrated that the OEIP delivery can be self-powered via piezoelectric energy harvester, that converts body motion in the biomedical applications [24]. Especially OEIPs used with plants would benefit from energy-autonomy without relying on external energy sources, reducing dependence on external power grids or batteries. With advances in sensors, energy-autonomy and automation, OEIPs could harvest energy from the environment (e.g. rainfall, wind) and automatically trigger the electrophoretic delivery of molecules based on environmental conditions at favorable times for plant absorption.

To unlock portable and on-demand OEIP applications at the plant level, a portable, multisource and versatile energy source is needed. Here, we employed the mechanism of contact, or tribo-electrification, occurring on the surface of plant leaves in combination with tailored artificial leaves as a point-of-use energy source for small electronics, e.g. sensors, in remote environments as presented in detail in previous studies [25–28]. Energy conversion is achieved by translating the mechanical energy from passive motion like fluttering of leaves into transient contacts between the plant leaf and an artificial leaf made of silicone elastomers with an internal transparent electrode. The contact events lead to the formation of static surface charges by the triboelectric effect, and it was shown that the combination of silicone and plant leaves enhance the charge formation [28]. Separation after contact promotes the induction of the charges into the plant tissue acting as ion-conductive electrode and into the transparent electrode in the artificial leaf. [25–28] The charges can then be harvested from the plant tissue and the artificial leaf. Here, our analysis focuses on driving an OEIPs with such energy harvesters directly, without further energy storage and control elements.

We applied the artificial leaves on *Ficus altissima robusta* and converted wind energy into electricity to prove the feasibility to directly power the OEIP. The functionality of the OEIP powered by the artificial leaves was demonstrated by delivering protons into a pH indicator solution of methyl red causing a quantitative color change as function of the delivered proton concentration from yellow (pH above 7) to red (pH below 6.2). This pH indicator allows qualitative monitoring of the experiments by the naked eye and a straightforward quantification of the delivered protons.

2. Materials and methods

2.1. Plants preparation and artificial leaf fabrication

Two small plants of *Ficus altissima robusta* were selected to host the artificial leaves due to their large and mechanically stable leaves and petioles. The artificial leaves were prepared following the procedures described earlier [25]. In short, a silicone layer (500 μm) was glued onto an indium tin oxide (ITO) coated polyethylene terephthalate (PET) sheet (200 μm) and laser cut into the desired shape. The artificial leaf shape was chosen based on the *Ficus* leaf size and shape. One artificial leaf per plant was fixed on the petiole using parafilm. Then, a 0.6 mm gold-coated pin electrode was inserted in the plant stem, to harvest charges in the plant tissue and a cable was attached to the ITO electrode to harvest charges created on the artificial leaf as described earlier [25]. To rectify the AC signal generated by the leaf motion into a DC signal to drive the OEIPs, a standard diode bridge (MB4S, Vishay) was used and the OEIP was directly connected to the + and − outputs. No further electrical components were required for proof-of-concept operation.

2.2. OEIP fabrication

The capillary OEIPs were prepared as previously described [29], however in this study capillaries of smaller inner diameter were applied (25/150 μm ID/OD). Shortly, the capillaries were sequentially flushed with KOH, 3-(trimethoxysilyl)propyl methacrylate (10 wt% in toluene) and ethanol. Afterwards, the capillaries were filled with polyelectrolyte mix containing

monomer AMPS (50% wt% in DI water, Sigma-Aldrich), cross-linker polyethylene glycol diacrylate (molecular weight 575 g mol^{-1}, 2 wt%, Sigma-Aldrich), the two photoinitiators: 2-hydroxy-4′-(2-hydroxyethoxy)-2-methylpropiophenone (Irgacure 2959; 0.5 wt%, Sigma-Aldrich) and Lithium phenyl-2,4,6-trimethylbenzoylphosphinate (LAP, 0.5 wt%, Sigma-Aldrich). The monomers in the capillaries were photo-polymerized for 138 min using a photoexposure box with blue light DULUX L BLUE 18 (Osram, Sweden). The capillaries were trimmed into ∼1 cm long sections that were attached to tubing, that serve as the reservoir for the source electrolyte.

2.3. OEIP mediated H^+ delivery

The OEIP reservoirs were filled with 0.1 M aqueous HCl. The delivery tip was immersed in the target electrolyte (30 μl) that consisted of the pH indicator methyl red (2.5 mM; Sigma-Aldrich) and 0.01 M KCl (Sigma-Aldrich). The OEIP was loaded with H^+ ions by applying constant current of 100 nA with a Keithley 2602 source-meter, using two Ag/AgCl electrodes. Once the device was loaded, the artificial leaves were attached as described above to supply the voltage for the OEIP-mediated H^+ delivery. The H^+ delivery triggered color changes of the pH indicator from yellow to red at pH below 6.2. Every experiment was typically repeated 3 times thus yielding 3 datapoints for analysis.

2.4. Quantification of H^+ and K^+ concentration in the target electrolyte

The delivered H^+ concentration was determined using pH meter (Orion 211, Thermofisher) with a H^+ or K^+ half-cell Ion Selective Electrode (Mini 4.6; NT Sensors, Spain) and a reference electrode (Ag/AgCl). The measured [H^+] concentrations were adjusted to account for dilution and volumes losses during measurements. To analyze the colorimetric changes in the methyl red due to the H^+ delivery, the photometric spectrum of the target solution was acquired using Nanophotometer NP80 (Implen, Sweden). The pH meter was calibrated each day before the measurement, enabling quantitative assessments. The spectrophotometer was also calibrated but due to a fast bleaching of the methyl red after H^+ delivery, these results could be analyzed only in a qualitative manner. The potassium ion-selective electrode lacks calibration, thus results were only treated as indication that K^+ were delivered.

3. Results & discussion

The artificial leaf was realized in a three-layer structure consisting of a 200 μm PET base layer, followed by a ∼0.1 μm ITO layer acting as internal electrode, coated with a 500 μm silicone layer as reported earlier [28]. The key characteristic for energy harvesting is the silicone layer, as the material is known to enhance the creation of surface charges during transient, wind-driven contacts with plant leaves [28]. Charges are induced into the internal electrode when leaves separate during flapping motion.

The artificial leaves were fixed on plants of *Ficus robusta altissima* and exposed to continuous air flow supplied from a laboratory fan, simulating wind (figure 1), to generate power for the OEIP-mediated H^+ delivery. Every wind-driven contact of the artificial leaf produces charges on both surfaces, the surface of the natural and artificial leaf, while every separation leads to charge separation and electrostatic induction of the charges of opposite polarity in the artificial leaf electrode and inner ion-conductive tissue, respectively, thus creating an alternating current [25]. To harvest these charges, an electrode was connected to the artificial leaf and a 0.6 mm gold-coated pin electrode was inserted into the tissue of the plant at the stem. The two electrodes produce alternating current signal and were thus connected to a bridge rectifier external to the tissue to generate a direct current driving the OEIP.

Figure 2(a) gives an overview of the charges generated by an artificial leaf with a *Ficus robusta* at two different wind speeds (voltage and current signals under same conditions are given in supplementary figure 1). The mean amplitude of the charge peaks is 16.7 ± 4.8 nC at 2.4 m s^{-1} and 27.0 ± 4.5 nC at 3.3 m s^{-1}, respectively. Moreover, an 69% increase of the frequency of the peaks is observed (∼100 peaks 2.4 m s^{-1} and 169 peaks at 3.3 m s^{-1}) due to augmented vibrations at higher wind speeds. The signal amplitude and frequency are expectedly wind speed dependent as also previously shown for similar systems [25, 27].

Figure 2(b) presents the characteristic rectified current and voltage output of two artificial leaves used for powering OEIPs, each consisting of the plant with a single artificial leaf each under the experimental conditions: a wind speed of 3.3 m s^{-1}, a temperature of 21 °C, and 17.2% relative humidity, details are given in supplementary figure 2. These are realistic conditions that would likely occur also in an outdoor environment. The daily mean wind speeds in Europe are typically below 3–4 m s^{-1} especially on lower heights (e.g. 10 m above ground level) and leaves show significant motion already at 1 m s^{-1} [27]. In previous work, a mechanical-to-electrical energy conversion efficiency of up to 0.14% has been reported for a similar triboelectric system using contact between leaf and silicone elastomer [26]. Factors like the effective contact area, the impact force, the environment (e.g. wind speed and humidity) affect the energy conversion efficiency thus we kept the environmental conditions constant to focus our experiments on the proof-of-concept of driving the OEIP.

It was observed that the current and voltage output remained comparable between the two plants. For the plant with artificial leaf 1, the median of

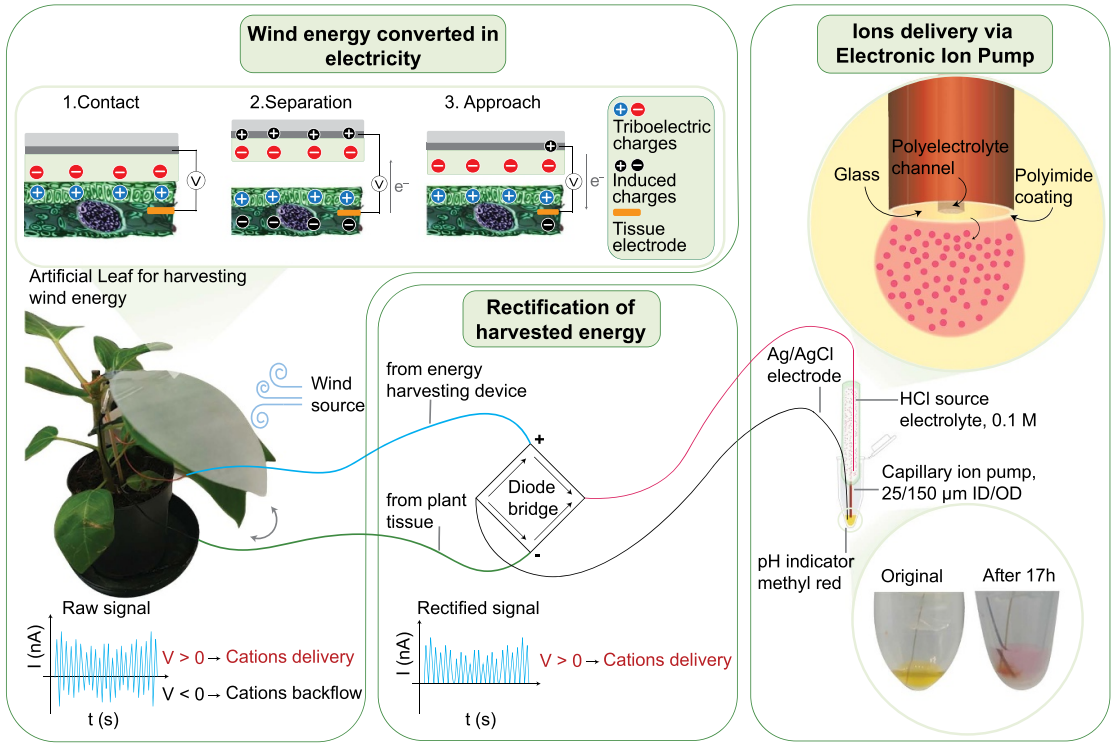

Figure 1. Overview of the organic electronic ion pump (OEIP) powered by the plant-hybrid triboelectric generator harvesting energy from the leaf motion in wind. The operation is divided into three panels: (left panel) conversion of the wind energy into electricity using plant and artificial leaf motion; (middle panel) rectification of the AC output of the energy harvesting to promote efficient delivery to target electrolyte; and (right panel) proof-of-concept delivery of protons to the pH indicator target through the use of OEIP.

the instantaneous current peaks is 164 nA and the median of the voltage peaks is 12 V. To obtain an estimate of the peak power, we multiplied the medians ($P_{\text{peak}} = V_{\text{peak, median}} \times I_{\text{peak, median}}$) resulting in 1.97 μW. For the plant with artificial leaf 2, the instantaneous current peaks have a median of 120 nA, the voltage peaks of 26 V (peak power estimate of 3.12 μW), as given in figure 2(b). The average power was estimated instead using the root mean square (RMS) of current and voltage signals resulting in 0.21 μW and 0.59 μW for plants with artificial leaf 1 and 2, respectively. Further analysis of power outputs of similar plant-hybrid harvesters as function of wind speed, artificial leaf design, contact area, has been reported earlier [25, 27]. The observed variations of the estimated peak power within less than an order of magnitude are expected due to the natural differences in the plant structure, the leaf size and shape, and the complex dynamic conditions when actuated in wind.

As the alternating contact and separation motion creates an AC voltage, typical for triboelectric generators (see inset in figure 1), the signal was rectified using a standard diode bridge rectifier as the negative voltage peaks would otherwise drive cations in the OEIP backflow, i.e., deliver from the target to the source electrolyte. As such, cation delivery (here: H^+) from the source electrolyte to the target electrolyte at each positive voltage peak is expected and accordingly observed as described later.

The rectified current is then used to power the OEIP via Ag/AgCl electrodes as connections. To characterize and verify the functionality of the assembled OEIP devices, the resistance when delivering H^+ from the source electrolyte to the methyl red target was measured. For applied constant current of 100 nA, the devices had stable voltage characteristics with an average voltage between 0.4 and 0.7 V therefore confirming the device operation and H^+ delivery (figure 2(c)).

Next, the OEIPs were powered for several hours in continuous operation using the artificial leaf as the only power source at an air flow of ~3.3 m s^{-1}. After 7 h of operation (figure 3(a); orange squares) and OEIP H^+ delivery, a red cloud close to the delivery tip started to become visible, signifying that protons have been delivered through the capillary and triggered a local pH decrease in the target solution (photos in figure 3(a)).

The concentration of the delivered H^+ ions was analyzed with a pH meter (figure 3(b)) and (a) spectrophotometer in parallel in order to determine the triggered colorimetric changes. The ratio of the yellow to red absorption peak is given in figure 3(a). It was observed that after the delivery, the protonated

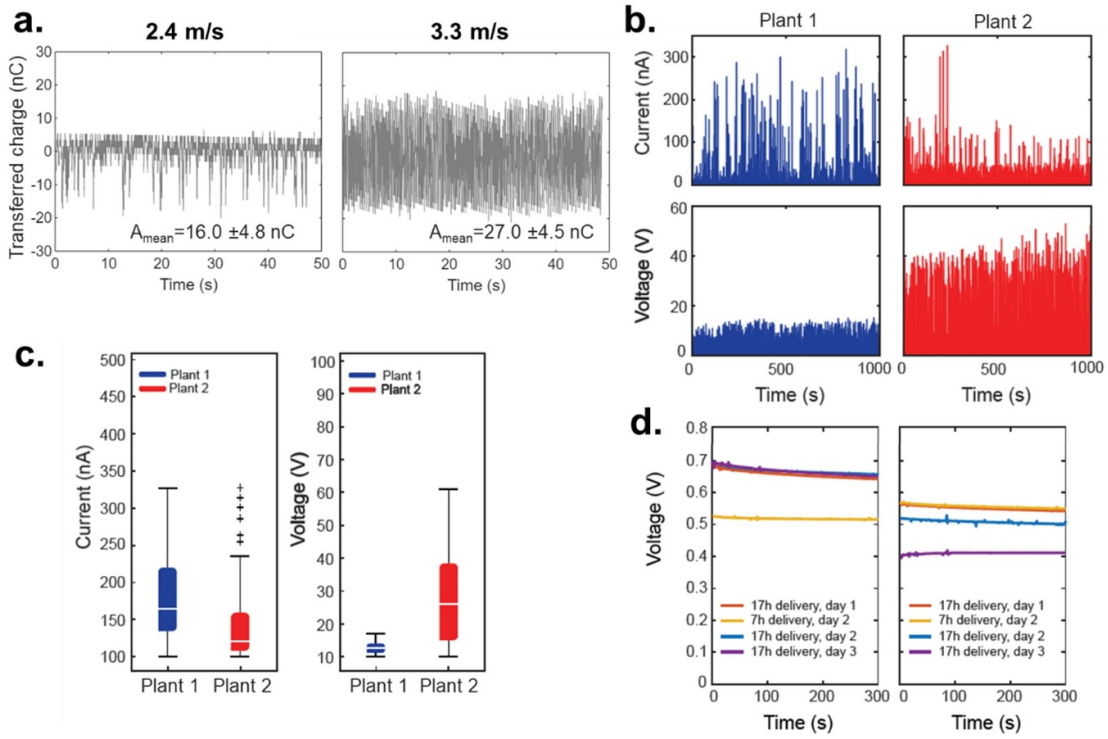

Figure 2. Charge formation and characteristics of plant-hybrid generators for powering the OEIPs. (a) Charges generated by an artificial leaf installed on a *Ficus robusta* at two different wind speeds (A_{mean} indicates the mean amplitude of the charge peaks), current and voltage signals are given in supplementary figure 1. (b) Rectified current and voltage signals of the two plants with artificial leaves 1 and 2 used to power the OIEPs and (c) box plots summarizing peak current and voltage signals. The boxplot top and bottom edges indicate the 75th and 25th percentile, respectively; the midline in the box identifies the median; the error bars indicate the minimum and maximum values while the '+' symbols represent the outliers. (c) Voltage characteristics of OEIPs when sourcing constant current of 100 nA during the delivery of H^+ to methyl red target electrolyte; different colors indicate same devices characterized after different experiments.

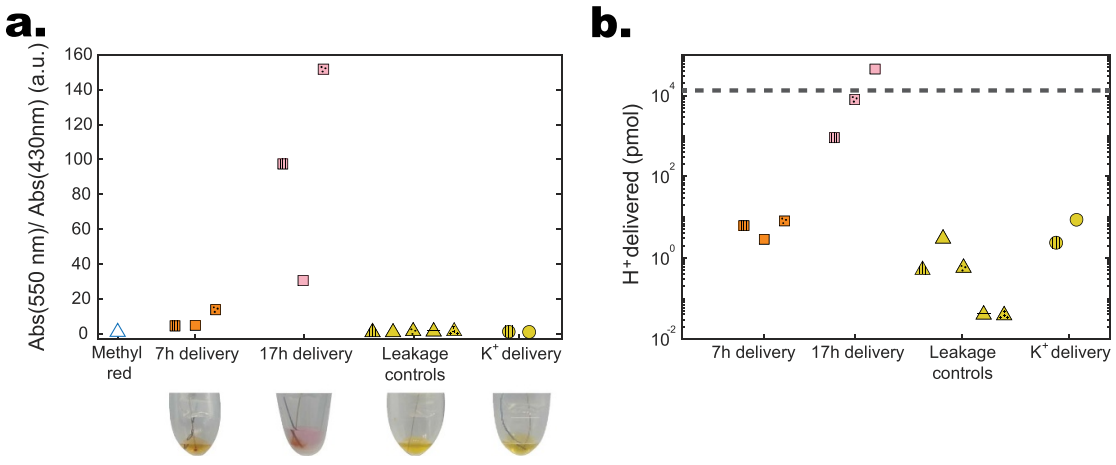

Figure 3. Artificial leaf triboelectric nanogenerator powers OEIP-mediated H^+ delivery (wind speed of 3.3 m s^{-1}, T = 21 °C, RH 17.2%). (a) Analysis of the colorimetric changes of the pH indicator after the experiments as the ratio of the absorbance bands at 550 nm (red) and 430 nm (yellow). At the bottom, pictures of the solutions at the end of the delivery for each class. (b) Number of moles of delivered H^+ to methyl red pH indicator determined using pH meter. The dashed line indicates the theoretical delivery estimated using the extrapolated charges generated in 17 h by the plant-hybrid generators (average of artificial leaf 1 and 2). In both graphs, each symbol represents a single sample; typically, three experiments were carried out for each experimental condition.

methyl red bleaches quickly (supplementary figure 3), thus spectrometric analysis serves only as a qualitative indication. Yet, the H^+ concentration measured with the pH meter gave stable and quantitative indications. After 17 h of continuous wind energy conversion and charge transfer to the OEIPs, significant color changes were observed, turning the solutions from yellow to pink/red. Moreover, the pH measurements (pink squares) indicated delivery of up to 44 nmol of H^+ confirming the operability of the OEIP with the

artificial leaf. The amount of the delivered H^+ during 7 h triboelectric nanogenerator (TENG)-operation was too low to affect the resulting pH and absorption spectrum of the target solution.

The electrophoretic velocity $v = \mu E$ of the delivered molecules is proportional to the electric field with the strength $E = V/d$, where V is the voltage, d the distance between the electrodes, and μ is the electrophoretic ion mobility (depends on the molecule's charge, size, and the medium). As the voltage increases, the electric field strength increases, leading to a proportional increase in the speed of molecular movement. Assuming a mobility of protons in water of 3.6×10^{-7} m^2 V s^{-1} (at 25 °C), an RMS voltage of 5.5 and 19 V (artificial leaf 1 and 2, respectively), and an electrode distance of 0.02 m, this results in v of 10^{-4} and 3.4×10^{-4} m s^{-1}, respectively.

To estimate the system efficiency, we have determined the charge delivered by both plants (with artificial leaf 1 and 2, respectively) as integral of current–time plot (figure 2(a)) over the 1000 s and extrapolating results to 17 h delivery. This results in 0.0012 C and 0.001 C (plants with artificial leaf 1 and 2, respectively). In the ideal case, each generated charge could enable the OEIP-mediated delivery of one H^+. Dividing the extrapolated charge by the Faraday constant, 96 485 C mol^{-1}, theoretically, 12.4 nmol and 10.4 nmol delivery could be expected during 17 h of TENG operation for plants with artificial leaf 1 and 2, respectively (dashed line in figure 3(b)). Indeed, we measured that the TENG-powered OEIP delivered 17.8 ± 23.5 nmol of H^+ ions, matching well the theoretical values. The system delivered even more H^+ (44 nmol in one case) than predicted indicating that extrapolation and restrictions in current sampling frequency may not fully capture current peaks, omitting charges available for ion transfer. Furthermore, alternating current peaks may facilitate enhanced H^+ delivery even at zero-current intervals, driven by the steep H^+ concentration gradient between the target electrolyte and the H^+-loaded OEIP membrane.

The variation in the obtained results could be related to natural differences in leaf sizes and shapes, which lead to variations in the harvested energy [30], for example, due to a variation in the effective contact area resulting in slightly differing delivery characteristics, while remaining acceptably reproducible for our proof-of-concept study. Elevating charge generation by maximizing factors such as contact area through artificial leaf design [27] could be strategies to further improve the systems.

To verify whether the delivery of protons was a result of the current produced by the artificial leaves, several control experiments were performed. The contribution of a potential H^+ diffusion leakage from the source electrolyte was evaluated by setting up the system in the same manner but disconnecting it from the energy harvester (yellow triangles in figures 3(a) and (b)). After 17 h, the target solutions were still yellow, and the pH was 8 as in the untreated methyl red, indicating that no protons had been delivered through a leakage.

A second control experiment was performed to determine whether electric field-enhanced water splitting contributed to the H^+ increase, as the artificial leaf may generate sufficient voltages, of up to 40 V, which could lead to side reactions [21]. To test this hypothesis, the OEIPs were connected to the artificial leaf exposed to air flow, but the source electrolyte was KCl instead of HCl. If water splitting was indeed taking place, then the resulting protons would be generated in the KCl solution and turn the target solution pink. Yet, when the OIEPs were operated for 17 h with KCl as source electrolyte neither a colorimetric change, nor a pH change of the methyl red target were observed confirming that H^+ generation through water electrolysis did not occur under these conditions. Instead, in two independent experiments the K^+ delivery was confirmed via K^+ ion selective electrode that showed the voltage increase from 48 mV to 68 and 72 mV.

A third control experiment was performed to evaluate a potential effect of noise caused by radiofrequency radiation (RF). The reason behind this control is that plants may act as receiving antennas that can absorb and harvest RF energy from the environment. Using a similar circuitry, as in our experiments, it has been reported to be able to charge capacitors independent of exposure to wind [26]. Thus, a subset of experiments was replicated inside a Faraday cage (current and voltage characteristics are reported in supplementary figure 4), while the remaining experiments were carried out without shielding the plant from the RF noise of the laboratory environment. The results given in supplementary figure 5 (and indicated with the tag 'wind only') show that the number of protons delivered in air flow in the Faraday cage is very similar compared to the experiments conducted in air flow outside the electric field shielded zone. As a further proof, OEIP devices were connected to a plant that was not exposed to an air stream (no leaf movement), outside of a Faraday cage and with all the electrical equipment in the laboratory that could cause RF noise switched on. The target solutions, indicated with the label 'RF only', did not show any color change even after 17 h, thus the delivery of protons is considered insignificant or very low. As such, the evaluation of the influence of RF on the outcome excluded a significant contribution of RF energy under the experimental conditions.

These results confirm that the TENG-powered OEIP enables significantly higher H^+ ion delivery than all control tests described below, validating autonomous powering and ion transport with a single leaf at a wind speed of 3.3 m s^{-1}. As mentioned above, the ion delivery depends on power output and charge quantity, which is a function of the

artificial leaf's energy conversion efficiency, and parameters like wind speed, effective contact area, and environmental conditions. A detailed comparison of the power output of plant-hybrid energy harvesters, based on the same mechanism, with other energy harvesters and the energy consumption of electronics can be found in the literature [26, 27]. In combination with the OEIP, only a bending-operated piezo electric energy harvester has been used before in a biomedical context (output voltage of 170 V, short circuit current 1.9 μA, peak power 300 μW) [23]. Importantly, our system can directly convert wind-induced passive leaf fluttering into electricity using relatively simple materials, unlike bending-driven harvesters. Even when achieving only 2–3 μW peak power, this is enough to power the OEIP with a single leaf. Moreover, our system is less complex and does not use an energy storage and control circuit but uses the charges directly.

The molecular delivery through the OEIP is fully driven by wind and is tailored to activate the delivery unit during sufficient wind which means on the other hand that delivery in still air is limited. This could be overcome by energy storage solutions and microcontrollers with additional power consumption, but other factors should be considered as well, e.g. that plant transpiration, photosynthesis and other physiologically relevant traits are affected by wind which could create situations that may be beneficial for simultaneous delivery of specific molecules.

A clear advantage over other wind energy harvesting systems is that the plant itself provides the mechanical structure to convert wind into electrical energy, reducing material costs and installation efforts. The transparent, soft artificial leaf is a minimal addition to the natural system and does not harm the plant or interferes with photosynthesis, further details in [25–28]. Moreover, the artificial leaves could be further advanced by systems capable to convert rain drops into electricity to further increase and diversify the power generation capability [31].

4. Conclusions

This work demonstrates that an ionic delivery device can be powered by harvesting the leaf motion energy using the triboelectric effect and minimal circuitry (only wires and a diode bridge). The OEIP effectively transports molecules autonomously from a source to a target electrolyte, utilizing the intermittent current peaks that accumulate ions over time. Several control tests were performed to ensure that the delivery of protons was powered solely by the wind-driven leaf motion. Future studies should also evaluate the long-term outdoor performance and power metrics of these systems.

This artificial leaf-powered OEIP system can operate autonomously using wind, and holds promise for delivering advantageous molecules to plant tissue, such as plant hormones or biostimulants, to enhance nutrient efficiency, stress tolerance, or crop quality and yield. Expanding this design to include additional circuit components or customized software, as demonstrated in prior work [31], could enable to trigger delivery under specific conditions, broadening potential application scenarios. With straightforward modifications [31], this system could be also coupled with other environmental energy sources, such as rain.

Data availability statement

The data that support the findings of this study are openly available at the following URL/DOI: https://doi.org/10.48557/RNW2D3.

Acknowledgments

IBW, AMD and ES acknowledge funding from the Swedish Foundation for Strategic Research (FFL18-0101) and the Swedish Government Strategic Research Area in Materials Science on Advanced Functional Materials at Linköping University (Faculty Grant SFO-Mat-LiU No. 2009-00971). SA, FM and BM acknowledge funding by the Project GrowBot, the European Union's Horizon 2020 Research and Innovation Programme under Grant Agreement No. 824074.

ORCID iDs

Serena Armiento https://orcid.org/0000-0002-0318-4250
Iwona Bernacka-Wojcik https://orcid.org/0000-0002-7135-8275
Abdul Manan Dar https://orcid.org/0000-0002-7573-6915
Fabian Meder https://orcid.org/0000-0002-1331-0265
Eleni Stavrinidou https://orcid.org/0000-0002-9357-776X
Barbara Mazzolai https://orcid.org/0000-0003-0722-8350

References

[1] Mikula K *et al* 2020 Controlled release micronutrient fertilizers for precision agriculture—a review *Sci. Total Environ.* **712** 136365
[2] Yin H, Cao Y, Marelli B, Zeng X, Mason A J and Cao C 2021 Soil sensors and plant wearables for smart and precision agriculture *Adv. Mater.* **33** 2007764
[3] Soussi A, Zero E, Sacile R, Trinchero D and Fossa M 2024 Smart sensors and smart data for precision agriculture: a review *Sensors* **24** 2647
[4] Dufil G, Bernacka-Wojcik I, Armada-Moreira A and Stavrinidou E 2021 Plant bioelectronics and biohybrids: the growing contribution of organic electronic and carbon-based materials *Chem. Rev.* **122** 4847–83
[5] Rouphael Y and Colla G 2020 Editorial: biostimulants in agriculture *Front. Plant. Sci.* **11** 40

[6] Sible C N, Seebauer J R and Below F E 2021 Plant biostimulants: a categorical review, their implications for row crop production, and relation to soil health indicators *Agronomy* **11** 1297
[7] Tarafder C, Daizy M, Alam M M, Ali M R, Islam M J, Islam R, Ahommed M S, Aly Saad Aly M and Khan M Z H 2020 Formulation of a hybrid nanofertilizer for slow and sustainable release of micronutrients *ACS Omega* **5** 23960–6
[8] Grillo R, Mattos B D, Antunes D R, Forini M M L, Monikh F A and Rojas O J 2021 Foliage adhesion and interactions with particulate delivery systems for plant nanobionics and intelligent agriculture *Nano Today* **37** 101078
[9] Sampathkumar K, Sampathkumar K, Xian Tan K, Tan K X, Chye Joachim Loo S and Loo S C J 2020 Developing nano-delivery systems for agriculture and food applications with nature-derived polymers *iScience* **23** 101055
[10] Shakiba S, Astete C E, Paudel S, Sabliov C M, Rodrigues D F and Louie S M 2020 Emerging investigator series: polymeric nanocarriers for agricultural applications: synthesis, characterization, and environmental and biological interactions *Environ. Sci. Nano* **7** 37–67
[11] Fincheira P, Hoffmann N, Tortella G, Ruiz A, Cornejo P, Diez M C, Seabra A B, Benavides-Mendoza A and Rubilar O 2023 Eco-efficient systems based on nanocarriers for the controlled release of fertilizers and pesticides: toward smart agriculture *Nanomaterials* **13** 1978
[12] Xin X, Judy J D, Sumerlin B B and He Z 2020 Nano-enabled agriculture: from nanoparticles to smart nanodelivery systems *Environ. Chem.* **17** 413–25
[13] Isaksson J, Kjäll P, Nilsson D, Robinson N, Berggren M and Richter-Dahlfors A 2007 Electronic control of $Ca^{2}+$ signalling in neuronal cells using an organic electronic ion pump *Nat. Mater.* **6** 673–9
[14] Waldherr L *et al* 2021 Targeted chemotherapy of glioblastoma spheroids with an iontronic pump *Adv. Mater. Technol.* **6** 2001302
[15] Simon D T, Gabrielsson E O, Tybrandt K and Berggren M 2016 Organic bioelectronics: bridging the signaling gap between biology and technology *Chem. Rev.* **116** 13009–41
[16] Williamson A *et al* 2015 Controlling epileptiform activity with organic electronic ion pumps *Adv. Mater.* **27** 3138–44
[17] Jonsson A *et al* 2016 Bioelectronic neural pixel: chemical stimulation and electrical sensing at the same site *Proc. Natl Acad. Sci.* **113** 9440–5
[18] Poxson D J *et al* 2017 Regulating plant physiology with organic electronics *Proc. Natl Acad. Sci.* **114** 4597–602
[19] Bernacka-Wojcik I *et al* 2019 Implantable organic electronic ion pump enables ABA hormone delivery for control of stomata in an intact tobacco plant *Small* **15** 1902189
[20] Bernacka-Wojcik I *et al* 2023 Flexible organic electronic ion pump for flow-free phytohormone delivery into vasculature of intact plants *Adv. Sci.* **10** 14
[21] Seitanidou M, Tybrandt K, Berggren M and Simon D T 2019 Overcoming transport limitations in miniaturized electrophoretic delivery devices *Lab Chip* **19** 1427–35
[22] Poxson D J, Gabrielsson E O, Bonisoli A, Linderhed U, Abrahamsson T, Matthiesen I, Tybrandt K, Berggren M and Simon D T 2019 Capillary-fiber based electrophoretic delivery device *ACS Appl. Mater. Interfaces* **11** 14200–7
[23] Pařízková B, Antoniadi I, Poxson D J, Karady M, Simon D T, Zatloukal M, Strnad M, Doležal K, Novák O and Ljung K 2022 iP & OEIP—cytokinin micro application modulates root development with high spatial resolution *Adv. Mater. Technol.* **7** 2101664
[24] Gabrielsson E O, Jung Y H, Han J H, Joe D J, Simon D T, Lee K J and Berggren M 2021 Autonomous microcapillary drug delivery system self-powered by a flexible energy harvester *Adv. Mater. Technol.* **6** 2100526
[25] Meder F, Thielen M, Mondini A, Speck T and Mazzolai B 2020 Living plant-hybrid generators for multidirectional wind energy conversion *Energy Technol.* **8** 2000236
[26] Meder F, Mondini A, Visentin F, Zini G and Crepaldi M 2022 Multisource energy conversion modes in minimally altered plants with soft epicuticular coatings energy *Environ. Sci.* **15** 2545–56
[27] Meder F, Armiento S, Naselli G A, Mondini A, Speck T and Mazzolai B 2024 Charge generation by passive plant leaf motion at low wind speeds: design and collective behavior of plant-hybrid energy harvesters *Bioinsp. Biomim.* **19** 5
[28] Meder F, Must I, Sadeghi A, Mondini A, Filippeschi C, Beccai L, Mattoli V, Pingue P and Mazzolai B 2018 Energy conversion at the cuticle of living plants *Adv. Funct. Mater.* **28** 1806689
[29] Parker D, Dar A M, Armada-Moreira A, Bernacka Wojcik I, Rai R, Mantione D and Stavrinidou E 2024 Biohybrid energy storage circuits based on electronically functionalized plant roots *ACS Appl. Mater. Interfaces* **16** 61475–83
[30] Armiento S, Mondini A, Meder F and Mazzolai B 2022 A plant-hybrid system for wind monitoring connected with social media *2022 IEEE 5th Int. Conf. on Soft Robotics (Robosoft)* (IEEE) pp 287–92
[31] Armiento S, Meder F and Mazzolai B 2023 Device for simultaneous wind and raindrop energy harvesting operating on the surface of plant leaves *IEEE Robot. Autom. Lett* **8** 2269–76